Original Article

http://dx.doi.org/10.3348/kjr.2012.13.3.265
pISSN 1229-6929 · eISSN 2005-8330
Korean J Radiol 2012;13(3):265-274

Korean Journal of Radiology
KJR

MRI Study on the Functional and Spatial Consistency of Resting State-Related Independent Components of the Brain Network

Bumseok Jeong, MD, PhD[1], Jeewook Choi, MD, PhD[2], Ji-Woong Kim, MD, PhD[3]

[1]Graduate School of Medical Science and Engineering (GSMSE), Korea Advanced Institute of Science and Technology, Daejeon 305-701, Korea; [2]Department of Psychiatry, Daejeon St. Mary's Hospital, The Catholic University of Korea College of Medicine, Daejeon 301-723, Korea; [3]Department of Psychiatry, College of Medical Science, Konyang University, Daejeon 302-718, Korea

Objective: Resting-state networks (RSNs), including the default mode network (DMN), have been considered as markers of brain status such as consciousness, developmental change, and treatment effects. The consistency of functional connectivity among RSNs has not been fully explored, especially among resting-state-related independent components (RSICs).

Materials and Methods: This resting-state fMRI study addressed the consistency of functional connectivity among RSICs as well as their spatial consistency between 'at day 1' and 'after 4 weeks' in 13 healthy volunteers.

Results: We found that most RSICs, especially the DMN, are reproducible across time, whereas some RSICs were variable in either their spatial characteristics or their functional connectivity. Relatively low spatial consistency was found in the basal ganglia, a parietal region of left frontoparietal network, and the supplementary motor area. The functional connectivity between two independent components, the bilateral angular/supramarginal gyri/intraparietal lobule and bilateral middle temporal/occipital gyri, was decreased across time regardless of the correlation analysis method employed (Pearson's or partial correlation).

Conclusion: RSICs showing variable consistency are different between spatial characteristics and functional connectivity. To understand the brain as a dynamic network, we recommend further investigation of both changes in the activation of specific regions and the modulation of functional connectivity in the brain network.

Index terms: *Resting state network; Default mode network; Independent component analysis; Consistency; Functional connectivity*

Received June 8, 2011; accepted after revision November 10, 2011.
This research was supported by the Original Technology Research Program for Brain Science through the National Research Foundation of Korea (NRF) funded by the Ministry of Education, Science and Technology (No. 2010-0029266: B.S.J.).
Corresponding author: Jeewook Choi, MD, PhD, Department of Psychiatry, Daejeon St. Mary's Hospital, The Catholic University of Korea College of Medicine, 520-2 Daeheung-dong, Jung-gu, Daejeon 301-723, Korea.
• Tel: (8242) 220-9020 • Fax: (8242) 221-4776
• E-mail: cjwcool@catholic.ac.kr

INTRODUCTION

The resting-state network (RSN) is a term referring to functional networks of brain regions that are active when an individual is not focused on the outside world. The RSN is characterized by coherent oscillations at a rate lower than 0.1 Hz among brain regions. Generally, the default mode network (DMN) comprises a set of brain regions including the cingulate cortex, hippocampus, and medial prefrontal and inferior parietal cortices and includes members of several RSNs (1, 2). The DMN is active during sleep (3, 4) and under anesthesia (5), as well as when at rest (6), but is not activated during passive viewing with a natural scene (7). The DMN can be measured using various

neurophysiological or functional neuroimaging tools such as electroencephalography (EEG) (8), magnetoencephalography (MEG) (9, 10), functional magnetic resonance imaging (fMRI), and functional near infrared (fNIR) (11). The activity of the DMN detected with functional neuroimaging is similar to that of the electric or optic signal measured directly from the brain cortex (12, 13). While performing a task, the DMN shows a reciprocal relationship with the task-related active network (14). This means that the activity of the DMN may be decreased while performing a task and increased during the resting state. A previous study reported that the more extensive the cognitive task is, the more active the subsequent resting state of the DMN becomes (15). Thus, the RSN, including the DMN, might form part of the backbone of brain behavior.

It is understood that the DMN plays a role in cognitive processes such as self-reflection, moral reasoning, recollection, or imagining the future (6). The DMN may also be associated with some psychopathologies, (e.g., self-disturbance in schizophrenia) (16), and inattentiveness in attention deficit hyperactivity disorder (ADHD) (8, 17). In previous neuroimaging studies, deficits in the DMN have been reported in various neuropsychiatric disorders (18), including schizophrenia (10, 14), autism (19), ADHD (20-23), Alzheimer's-type dementia, and mild cognitive impairment (24-26). From a clinical perspective, a question of interest is whether a deficit in the DMN can be restored or modulated. Prior studies have reported that deficits in the DMN can be modulated with antipsychotic medication in schizophrenia (27) and with psychostimulants in ADHD (28, 29). These results suggest that the characteristics of the DMN may provide a measure of treatment effectiveness as well as confirmation of diagnosis. To measure the treatment effect, however, the characteristics of the DMN need to be consistent across time. Previous studies using the fMRI data of healthy individuals have reported the test-retest reproducibility of the spatial characteristics of the RSN including the DMN (30, 31). However, the reproducibility of the functional connectivity of the RSN, including the DMN, has not yet been established using fMRI data, even though the functional connectivity among resting-state-related independent components (RSICs) has been used to explore clinical significance (32).

Usually, the DMN is constructed using a correlation map between the time course of a seeding point or region of interest (ROI) and those of all other voxels within the brain (33, 34). This seed-based correlation analysis using anatomical ROIs could suffer from the confounding factor of individual anatomical variability (35), and could also show only relationships of one-to-multiple ROIs and not relationships among all ROIs. An alternative ways of constructing the DMN is to extract raw time-course data from the ROI selected on the spatial map of the independent component (IC) (32). However, the raw time courses might also be affected by various forms of noise, even though the seeding point was chosen based on the IC map. In the present study, the time courses of RSICs, rather than raw time courses, were used for measuring functional connectivity. Our approach might be less affected by either individual anatomical variability, as with a seed-based approach, or by noise, as with an ICA approach using raw time courses. Also, all connections among RSICs could be explored with our approach using the time courses of RSICs, unlike the seed-based correlation analysis. In this resting-state fMRI (rs-fMRI) study, we addressed the consistency of functional connectivity among the time courses of RSICs and also confirmed the spatial characteristics of RSICs in healthy individuals.

MATERIALS AND METHODS

Subjects

Enrollment for subjects was advertised on the message board at Eulji University Hospital, Daejeon, Korea. Thirteen healthy young male subjects (Age = 22.4 ± 2.5 years) underwent fMRI. Subjects were interviewed by a psychiatrist using DSM-IV criteria to exclude any possible psychiatric disorders. All subjects were right-handed and had no history of psychiatric or neurological disorders or head trauma. This study was approved by the institutional review board of the Eulji University Hospital. All subjects provided written informed consent before participation in the present study.

Functional MRI Experiments

Subjects underwent fMRI scan of 5 minutes and 30 seconds both on day one and after 4 weeks at rest with their eyes closed. Using 3.0 Tesla MRI (ISOL, Gwangju, Korea), fMRI was acquired with a BOLD-sensitive echo-planar gradient-echo (EPI) sequence with the following imaging parameters: repetition time (TR), 2000 ms; echo time (TE), 35 ms; flip angle (FA), 70°; spatial resolution, 3.4375 x 3.4375 x 5 mm^3, imaging matrix, 64 x 64; field-of-view (FOV), 220 x 220 mm^2, number of slices, 25, 165 volumes. Subjects were instructed to keep their eyes closed

Korean Journal of Radiology
KJR

and not to think of anything particular during fMR scans.

Data Preprocessing

The fMRI data were processed and analyzed using the MELODIC (Multivariate Exploratory Linear Optimized Decomposition into Independent Components) module of the FSL software (http://www.fmrib.ox.ac.uk/fsl/feat5/index). The first five scans were discarded to account for T1

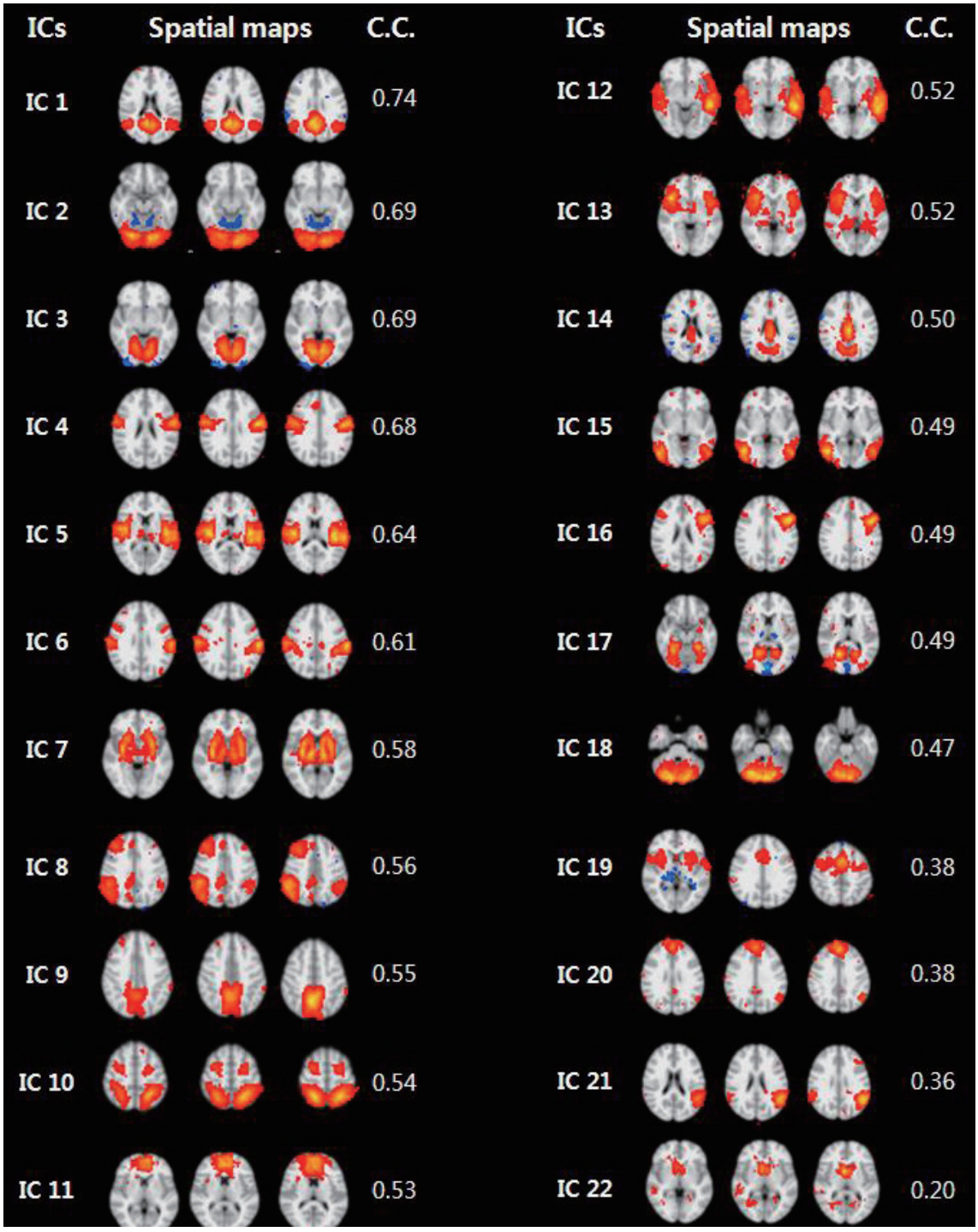

Fig. 1. 22 RSIC maps and their highest spatial correlation coefficients (C.C.) among possible 63 IC pairs between two time points (at day 1 and for after 4 week). Posterior default mode network (IC 1), visual system (IC 2, IC 3, IC 10, IC 15, IC 17), sensorimotor system (IC 4, IC 5, IC 6), subcortex (IC 7, IC 22), frontoparietal network (IC 8, IC 21), superior parietal network (IC 9), anterior default mode network (IC 11, IC 20), temporal network (IC 12), executive control system (IC 13, IC 14, IC 16), cerebellum (IC 18), motor system (IC 19), parietal network (IC 21).

saturation effects. The remaining 160 images were spatially realigned using a rigid-body transformation and were subjected to slice-timing correction. Next, a brain mask from the first fMR data volume was created to eliminate signals outside of the brain in each subject. Spatial smoothing using a full-width Gaussian kernel at half-maximum, 6 mm was performed to reduce noise without reducing valid activation. The smoothed images were filtered with a 128-second high pass filter to effectively remove signal drift. The serial correlations were removed to validate the statistics and be maximally efficient. Finally, the functional images were registered to the Montreal Neurological Institute (MNI) T1 template using FLIRT (FMRIB's Linear Image Registration Tool) for FSL.

Spatial Consistency of RSIC Maps Across Time

To test the spatial consistency, multisession temporal concatenation (36) was run on all 13 participants as a group at each time point where a standard (space x time) ICA decomposition was conducted. Both the principle-component analysis (PCA) and the subsequent ICA algorithm produced 54 ICs at week 0 and 63 ICs at week 4. Each IC map was divided by the standard deviation of the residual noise and was plotted onto a histogram of intensity values (37). MELODIC was used to carry out inference on the estimated maps using a Gaussian/gamma mixture model and an alternative hypothesis testing approach at a threshold level of 0.5. A threshold level of 0.5 in the case of alternative hypothesis testing means that a voxel survives thresholding as soon as the probability of it being in the active class exceeds the probability of it being in the background-noise class (37). The spatial cross-correlation analyses among 3402 IC pairs (54 x 63), between two time points, were performed with thresholded IC maps using FSL. This means that 63 correlation coefficients were produced for each of the 54 ICs on day 1. The IC pair showing the highest correlation coefficient among the 63 possible ICs was considered as the same IC between two time points and their correlation coefficients used for a value of spatial consistency. Among the 63 ICs, 41 were not RSICs were signals from white matter, cerebrospinal fluid, vessels, and motion artifacts. The remaining 22 pairs were selected as the RSIC and were ordered with their correlation coefficients (Fig. 1). The spatial correlation coefficients were compared between RSICs and non-RSICs using a p value < 0.05 as a significance threshold. While this approach provided the degree of spatial consistency of each IC, it did not provide its statistical difference between two time points.

Another method using a post-hoc regression analysis was employed to test the question about whether spatial maps of RSICs are consistent across time. Unlike the first ICA method performed for each time point individually, this multisession temporal concatenation (37) was run on both time points of all the 13 participant pairs as a group. Both the PCA and subsequent ICA algorithm yielded 48 spatial IC maps. Each IC map was thresholded by fitting a mixture model using the same method outlined above (37). Among 48 ICs, 26 that were not RSICs were discarded as signals from white matter, cerebrospinal fluid, vessels, and motion artifacts. The remaining 22 RSICs were selected for a pairwise group comparison (Fig. 2). For the pairwise group comparison, to identify differences in spatial characteristics of RSICs according to time point, we specified a temporal-design matrix, a subject-design matrix, and corresponding contrast matrices. Finally, a post-hoc regression analysis was performed on estimated time courses and subject modes at a statistical threshold level of $p < 0.05$.

The Consistency of Functional Connectivity Among Time Courses of RSICs Across Time

To extract the RSIC time courses, we used the 22 ICs selected in the prior step for spatial consistency using the Gaussian/gamma model. To identify subject-specific temporal dynamics within each individual's fMRI dataset, the full set of group-ICA spatial maps was used in a linear model fit against the separate fMRI data sets (38). This process produced time courses for each component and subject. Time courses of the 22 RSICs of each subject were selected for further functional connectivity analysis. Here, both cross-correlation (CC) and partial-correlation (PC) coefficients were used as measures of functional connectivity. These correlation analyses produced CC and PC matrices of 22 by 22 in each subject. The CC referred to the covariance between time courses of members in each IC pair. The PC referred to the correlation of time courses between two ICs after accounting for the relationship of each time course to the other 20 reference time courses.

To test the consistency of functional connectivity across time, two approaches were applied. First, using correlation coefficients for all IC pairs, the intraclass correlation coefficient (ICC) was calculated between the two time points. The correlation coefficient of each IC pair was averaged across all subjects. Then, 462 pairs excluding 22 self-pairs in the group-averaged coefficient matrix (22 by

Korean Journal of Radiology
KJR

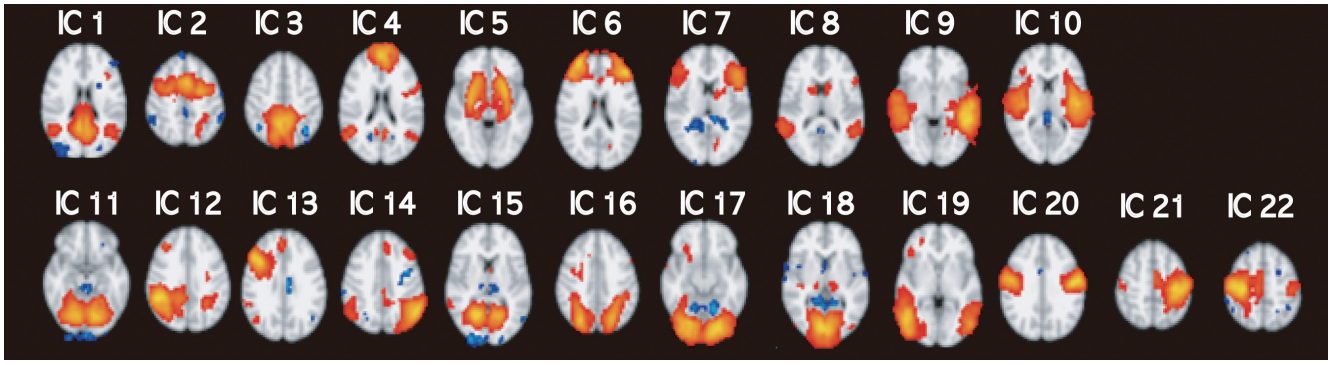

A

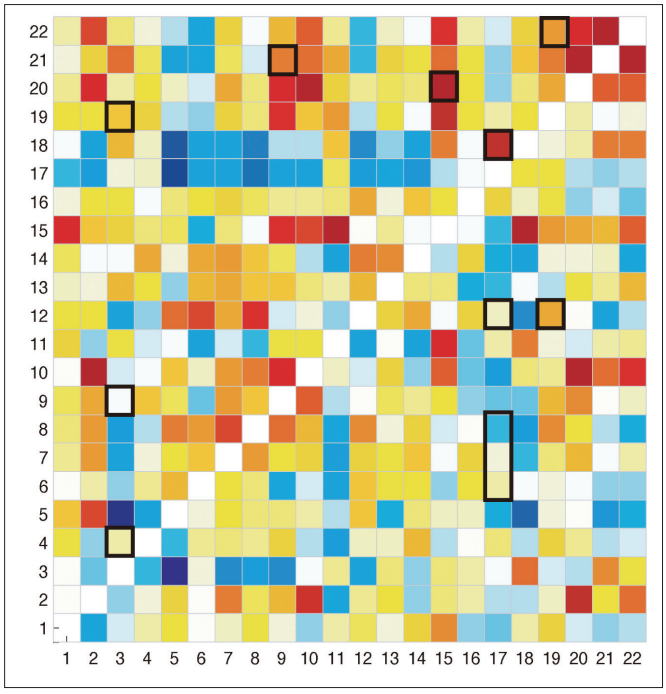

B

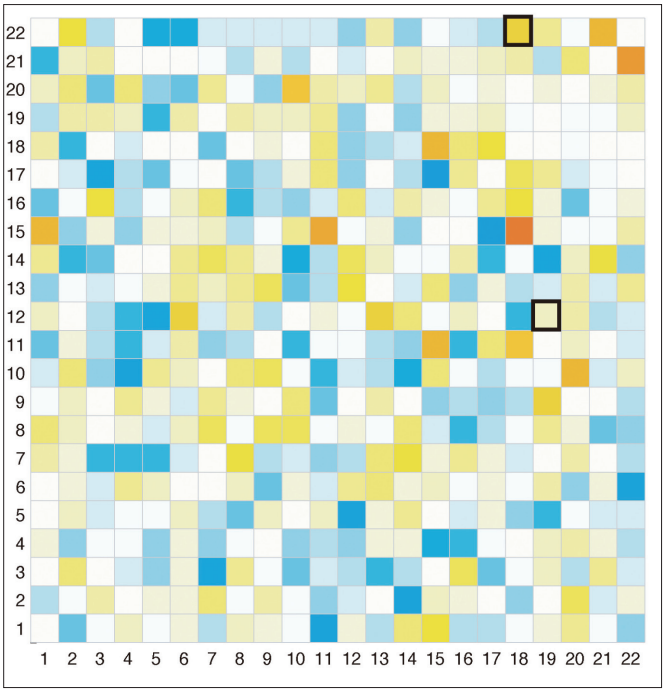

C

Fig. 2. Resting state related independent components (RSICs) and their functional connectivity maps.
RSICs (A). Functional connectivity maps for cross correlation **(B)** or partial correlation **(C)** among RSICs. In each diagonal matrix, left upper part of matrix represents functional connectivity map at day 1, while right lower part represents functional connectivity map after 4 weeks. Black-line box represents independent component pair, which showed significantly higher mean correlation coefficient in corresponding time point (e.g., black-line box in left upper part means that correlation coefficient is higher at day 1 than after 4 weeks).

22) were used to calculate the ICC. The Psych statistical package "R" (http://www.personality-project.org/r/html/ICC.html), was used to calculate the ICC between time points identified as "at day 1" and "after 4 weeks." The second approach was the comparison of the correlation coefficient of each IC pair between two time points. Fisher's r-to-z transformation was performed on the correlation coefficients. The z-transformed mean correlation coefficient of each IC pair was compared between "at day 1" and "after 4 weeks" using a paired *t* test at a statistical threshold level of $p < 0.05$. Corrections for multiple comparisons and false-discovery rate (FDR) were applied to the *p* values resulting from the paired *t* test.

RESULTS

Spatial Consistency

As a result of spatial cross correlation using FSL, 22 IC pairs showing the highest correlation coefficient between two time points were identified as RSICs. The spatial correlation coefficients among 22 RSICs ranged from 0.20 to 0.74 (0.53 ± 0.13) across RSICs (Fig. 1). The most spatially consistent RSIC was in the posterior cingulate cortex (PCC)/precuneus region known as a posterior DMN (39).

Relatively high spatial consistency was also found in the bilateral inferior occipital gyri (0.69), bilateral calcarine gyri (posterior medial visual component, 0.69), and bilateral precentral/postcentral gyri (0.68). RSICs showing relatively low spatial consistency were found in the basal ganglia (0.20), a parietal region of the left frontoparietal

Table 1. Spatial Consistency of Resting State Related Independent Components (RSICs) Using Results of Post-Hoc Regression Analysis

Network	IC	Regions	Voxels	Max(Z)	MNI Coordinates			Z Values	*P* Values
					X	Y	Z		
Post. DMN	1	L. Post. Cingulate C.	937	23.00	2	-46	28	0.83	0.20
		L. Angular G.		7.79	-46	-66	28		
		R. Angular G.		7.78	46	-58	32		
Motor S.	2	SMA	646	12.54	-26	-2	56	0.30	0.38
Sup. Parietal N.	3	B. Precuneus	763	14.48	-6	-54	60	0.42	0.34
Ant. DMN	4	L. Sup. Medial G.	810	10.80	2	54	28	-0.10	0.54
Subcortex	5	R. Putamen	1176	13.40	22	6	4	1.16	0.12
		L. Putamen		14.84	-22	6	8		
Executive control S.	6	L. Middle Frontal G.	271	9.41	-34	42	36	-0.56	0.71
		R. Middle Frontal G.	262	9.38	38	42	32		
	7	L. Inf. Frontal G.	399	14.30	-46	14	24	0.64	0.26
Parietal N.	8	L. SupraMarginal G.	264	13.7	-58	-50	32	0.85	0.20
		R. SupraMarginal G.	152	11	62	-42	28		
Temporal N.	9	L. Middle Temporal G.	732	15.00	-54	-38	-4	-0.11	0.54
		R. Middle Temporal G.	260	8.44	50	-34	-4		
	10	L. Rolandic Operculum/L. Sup. Temporal G.	656	15.70	-42	-22	16	-0.96	0.83
		R. Rolandic Operculum/R. Insula Lobe	333	12.50	42	-18	16		
Cerebellum	11	L. Lingual G./L. Cerebelum (VI)/L. Fusiform G.	869	15.70	-14	-74	-12	0.97	0.17
F-P N.	12	R. SupraMarginal G./Inf. Parietal Lobule/Angular G.	365	11.40	50	-46	36	1.08	0.14
	13	R. Inf. Frontal G.	322	12.90	42	22	32	0.61	0.27
	14	L. Inf. Parietal Lobule	554	18.30	-50	-58	48	1.10	0.14
		R. Inf. Parietal Lobule/Angular G.	50	7.32	46	-62	52		
		L. Inf. Frontal G. (p. Triangularis)	31	7.16	-50	26	28		
Visual S.	15	R. Calcarine G.	1145	21.40	22	-62	12	1.14	0.13
	16	R. Sup. Parietal Lobule/Angular G./ Sup. Occipital G.	539	14.2	26	-70	44	1.30	0.10
		L. Sup./Inf. Parietal Lobule	525	15.3	-26	-62	48		
	17	L. Inf. Occipital G./Fusiform G.	1287	19.20	-22	-86	-16	-0.84	0.80
	18	Bilteral Cuneus/Calcarine G.	1287	26.10	6	-86	8	0.55	0.29
	19	R. Middle Temporal/Occipital G.	632	17.20	54	-70	4	1.21	0.11
		L. Middle Temporal/Occipital G.	256	12.50	-50	-74	4		
Sensorymotor S.	20	L. Precentral/Postcentral G.	484	28.45	-50	-10	32	-0.95	0.83
		R. Precentral/Postcentral G.	435	22.70	50	-6	32		
	21	L. Postcentral/Precentral G.	738	15.80	-42	-30	60	0.58	0.28
	22	R. Precentral/Postcentral G.	708	18.60	38	-22	56	0.47	0.32

Note.— N = network, S = system, DMN = default mode network, SMA = supplementary motor area, Inf = inferior, Sup = superior, C = cortex, G = gyrus, L = left, R = right, B = bilateral

Korean Journal of Radiology
KJR

network (0.36), and the supplementary motor area (SMA) (0.38). The remaining 26 non-RSICs including physiological noise, non-gray matter signals, and motion artifacts showed significantly lower correlation coefficients (0.38 ± 0.17, *t* test, t = 3.58, df = 51.65, *p* = 0.001) than did the RSICs. The spatial correlation coefficients and the map of each RSIC are presented in the Figure 1.

In the post-hoc regression analysis with a mixed Gaussian/gamma model, the spatial characteristics of each RSIC pair were not significantly different between day 1 and after 4 weeks (z = 0.10-1.21, *p* = 0.10-0.90) (Table 1).

The Consistency of Functional Connectivity: ICC Across Time Interval

Intraclass correlation analysis showed that the correlation coefficients among all pairs of IC time courses were significantly consistent across the time interval. The ICC of CC was 0.78 (F = 7.93, *p* < 0.001, CI = 0.74-0.81), while the ICC of PC was 0.75 (F = 7.05, *p* < 0.001, CI= 0.71-0.79).

The Consistency of Functional Connectivity: Comparison of Mean Correlation Coefficients Across a Time Interval (Fig. 2)

CCs between several IC pairs were significantly different across a time interval. The CC was significantly decreased between IC3 (upper part of the precuneus) and IC4 (superior medial frontal gyrus: anterior DMN; t = 2.08, *p* = 0.05), IC9 (bilateral middle temporal gyri; t = 2.73, *p* = 0.01) or IC19 (bilateral middle temporal/lateral middle occipital gyri: V5; t = 2.13, *p* = 0.04). A decreased CC was also found for the IC12 (right angular and supramarginal gyri/intraparietal lobule) - IC19 pair (t = -2.20, *p* = 0.04). CC also significantly increased between IC17 (bilateral inferior occipital gyri) and IC6 (bilateral frontal poles/middle frontal gyri; t = -2.15, *p* = 0.04), IC7 (left inferior frontal gyrus; t = -2.23, *p* = 0.04), IC8 (bilateral supramarginal gyri; t =-2.48, *p* = 0.02), and IC12 (t = -2.29, *p* = 0.03). Increased CCs were also found for pairs IC9-IC21 (left precentral gyrus) (t = 2.49, *p* = 0.01) and IC15 (bilateral calarine gyri: anterior medial visual component) - IC20 (bilateral precentral/postcentral gyri) (t = 2.15, *p* = 0.04). In terms of PCs, the functional connectivity was significantly decreased in the IC12 - IC19 pair (t = -2.13, *p* = 0.04) and increased in the IC18 (bilateral cuneus/calcarine gyri: posterior medial visual component) - IC22 (right precentral/postcentral gyrus) pair (t = 2.63, *p* = 0.01). The functional connectivity, both for CC and PC, of the precuneus/posterior cingulate cortex component (IC 1, posterior DMN) with other RSICs, did not significantly change over 4 weeks. The differences in CC or PC disappeared after the correction for multiple comparisons using FDR.

DISCUSSION

This rs-fMRI study evaluated the consistency of both functional connectivity and spatial characteristics between 'at day 1' and 'after 4 weeks' among RSICs. First, we confirmed the spatial consistency of RSICs (30, 31) using two different methods: correlation analysis and the Gaussian/gamma model. Also, we found that spatial consistency was variable across RSICs. Second, our high intraclass correlation coefficient (ICC) result suggested that the overall functional connectivity among RSICs is consistent across time. However, in the comparisons of the correlation coefficients of each IC pair across time, the functional connectivity of several RSIC pairs was variable across time. Finally, RSIC pairs showing differences were more frequent in the cross-correlation (CC) analysis using Pearson's coefficient than in the PC analysis. Thus, our results suggest that both the spatial map and functional connectivity are consistent across time, but that the degree of their consistencies is variable across RSICs or by the correlation analysis method.

Our results regarding the spatial consistency of RSICs are consistent with previous results. We should also note that the spatial consistency was variable across RSICs (40), although they were more spatially consistent than were non-RSICs. Relatively high consistency was found in the posterior DMN, bilateral inferior occipital gyri, bilateral calcarine gyri (posterior medial visual component), and bilateral precentral/postcentral gyri, whereas relatively low consistency was found in the basal ganglia, parietal region of the left frontoparietal network, and supplementary motor area (SMA) (Fig. 1). A previous study using ICA also reported both variability of spatial consistency and relatively high spatial consistency of RSICs compared with non-RSICs (31). In that prior study, RSICs showing relatively high consistency were the bilateral frontoparietal network, bilateral occipital poles (bilateral inferior occipital gyri), posterior DMN, bilateral inferior frontal gyri, and bilateral supramarginal gyri, whereas the cerebellum, SMA, and basal ganglia had low consistency. The spatial consistency of most RSICs in the present study was similar to this prior study, in which the sessions were 45 min or 11 months

apart. Both the present and the prior studies suggest that DMNs are spatially reproducible and that the low spatial consistency of RSICs in both SMA and basal ganglia should be further investigated in a longitudinal study. The low spatial consistency of the frontoparietal network, especially in the left parietal region, was not consistent with the prior study. However, there has been an rs-fMRI study supporting our results (41), and they reported a systematic impairment of associative frontoparieto-cingulate areas in altered states of consciousness. The discrepancy between these studies regarding spatial consistency in the frontoparietal network, especially in the left parietal region, should be investigated using a high-dimensional ICA analysis, which could separate the frontoparietal network into frontal and parietal regions.

We also note the variability of functional connectivity in several RSICs, as well as the overall consistency of RSICs across time. In our study, the RSIC pairs showing differences in functional connectivity were mainly the connections within visual RSICs or between visual and other RSICs (Fig. 2). A MEG study has also shown that graph metrics of functional connectivity were generally consistent but that the reliability was variable across the frequency band (42). A recent rs-fMRI study using Pearson's CC analyses among raw time courses found that the correlation between the DMN and the 'anticorrelated' network of the resting-state network can vary over time (43). Thus, the functional connectivity of the resting-state brain network may be dynamically changed, yet may be consistent with the exception of a few RSIC pairs when functional connectivity is averaged within a certain period. The RSIC pairs showing the differences across time were more frequent in the CC analysis using Pearson's coefficient than in the PC analysis. Moreover, functional connectivity of the anterior DMN was variable across time in CC, but not PC. Furthermore, in CC, but not in PC, the upper part of the precuneus and inferior occipital gyri (occipital pole) showed differences in functional connectivity with multiple RSICs across time. This suggests that a possible indirect effect of functional connectivity among other RSICs on the functional connectivity of a certain RSIC pair can be controlled for using a PC analysis. A functional connectivity study using simulated fMRI data reported that a PC analysis was more reliable than a CC analysis (35). Consequently, the PC results are preferable in the present study. Interestingly, in both the PC and CC analysis, functional connectivity decreased across time between IC 12 (right angular and supramarginal gyri/intraparietal lobule) and IC 19 (bilateral middle temporal gyri). IC 19 comprises bilateral V5 areas with connectivity to V1 and V2 and the inferior and medial temporal gyrus. IC 19 is a region of the extrastriate visual cortex and is thought to play a role in the perception of motion and the guidance of some eye movements (44). In an fMRI study on a blind cohort, dorsal occipito-temporal regions were activated during the detection of auditory motion (45). The activated area in blindness was close to the maximum intensity point of IC 19 in the present study. Also, IC 12 was connected to the angular and supramarginal gyri and the visual cortex, consisted primarily of the parietal component of the right fronto-parietal network. The functional connectivity between IC 18 (posterior medial visual component) and IC 22 (right precentral/postcentral gyrus) was also variable in the PC analysis. Thus, there are some possible explanations for the variable functional connectivity of these visual information-process-related RSICs. Even if subjects have been asked to close their eyes, they could sometimes open their eyes, roll their eyeballs, or engage in visuospatial processing of scanner-induced noise during fMRI scanning. Their possible brain activity could modulate the functional connectivity of visual information-process-related RSICs. When subjects underwent fMRI scanning again, they might be less exploratory and more comfortable with their environment. If so, their functional connectivity under the relatively unfamiliar environment at day one could be reduced at 4 weeks. This may be a reason that the negative (IC 12-IC 19: bluish) or positive (IC 18-IC 22: yellowish) functional connectivity among RSICs 'at day 1' was not significant (whitish) at the 'after 4 weeks' time point in the present study (Fig. 2C). Our study showed no difference in functional connectivity across time after performing the correction for multiple comparisons. This should be not interpreted as implying that all functional connections are consistent. Rather, we argue that the correction for multiple comparisons should be applied in functional connectivity studies to reduce the possible false-positive error rate.

In our study, none of the RSICs showed inconsistency in either functional connectivity or spatial characteristics. However, in a disordered brain, the intensity of the change could be different between functional connectivity and the activation intensity of brain regions in a network. Thus, to understand the brain as a dynamic network, we would recommend the investigation of the modulation of functional connectivity in brain networks as well as the change in activation of the brain regions.

Korean Journal of Radiology
KJR

We should note some limitations of the present study. The spatial map of the identified RSICs could be slightly different at every ICA analysis, and thus their functional connectivity could be variable as well. Our results could be confirmed by ICA at various dimensions in a further study, as the number of RSICs produced by ICA differs according to the magnitude of the dimension used for data reduction. Inter-subject variance in areas such as mental status during scan, education, or intelligence might cause different functional connectivity among RSICs. Thus, our results require confirmation with a dataset from a large sample, even though one study verified ICA repeatability using 42 RSICs (46). The neuropsychological or clinical meaning of the functional connectivity of each IC pair should be explored in further studies.

We found that most of the RSICs were reproducible across time, whereas some RSICs were variable in both their spatial characteristics and functional connectivity. Functional connectivity might be affected by the correlation analysis method applied. Our results suggested that researchers should consider both the variability of functional connectivity among the RSICs across time and the influence of the correlation analysis method.

REFERENCES

1. Fox MD, Raichle ME. Spontaneous fluctuations in brain activity observed with functional magnetic resonance imaging. *Nat Rev Neurosci* 2007;8:700-711
2. Greicius MD, Srivastava G, Reiss AL, Menon V. Default-mode network activity distinguishes Alzheimer's disease from healthy aging: evidence from functional MRI. *Proc Natl Acad Sci U S A* 2004;101:4637-4642
3. Dang-Vu TT, Schabus M, Desseilles M, Albouy G, Boly M, Darsaud A, et al. Spontaneous neural activity during human slow wave sleep. *Proc Natl Acad Sci U S A* 2008;105:15160-15165
4. Horovitz SG, Braun AR, Carr WS, Picchioni D, Balkin TJ, Fukunaga M, et al. Decoupling of the brain's default mode network during deep sleep. *Proc Natl Acad Sci U S A* 2009;106:11376-11381
5. Greicius MD, Kiviniemi V, Tervonen O, Vainionpää V, Alahuhta S, Reiss AL, et al. Persistent default-mode network connectivity during light sedation. *Hum Brain Mapp* 2008;29:839-847
6. Gusnard DA, Raichle ME, Raichle ME. Searching for a baseline: functional imaging and the resting human brain. *Nat Rev Neurosci* 2001;2:685-694
7. Kim GW, Jeong GW, Kim TH, Baek HS, Oh SK, Kang HK, et al. Functional neuroanatomy associated with natural and urban scenic views in the human brain: 3.0T functional MR imaging. *Korean J Radiol* 2010;11:507-513
8. Helps S, James C, Debener S, Karl A, Sonuga-Barke EJ. Very low frequency EEG oscillations and the resting brain in young adults: a preliminary study of localisation, stability and association with symptoms of inattention. *J Neural Transm* 2008;115:279-285
9. de Pasquale F, Della Penna S, Snyder AZ, Lewis C, Mantini D, Marzetti L, et al. Temporal dynamics of spontaneous MEG activity in brain networks. *Proc Natl Acad Sci U S A* 2010;107:6040-6045
10. Rutter L, Carver FW, Holroyd T, Nadar SR, Mitchell-Francis J, Apud J, et al. Magnetoencephalographic gamma power reduction in patients with schizophrenia during resting condition. *Hum Brain Mapp* 2009;30:3254-3264
11. Zhang H, Duan L, Zhang YJ, Lu CM, Liu H, Zhu CZ. Test-retest assessment of independent component analysis-derived resting-state functional connectivity based on functional near-infrared spectroscopy. *Neuroimage* 2011;55:607-615
12. Arieli A, Shoham D, Hildesheim R, Grinvald A. Coherent spatiotemporal patterns of ongoing activity revealed by real-time optical imaging coupled with single-unit recording in the cat visual cortex. *J Neurophysiol* 1995;73:2072-2093
13. Shmuel A, Leopold DA. Neuronal correlates of spontaneous fluctuations in fMRI signals in monkey visual cortex: implications for functional connectivity at rest. *Hum Brain Mapp* 2008;29:751-761
14. Jeong B, Kubicki M. Reduced task-related suppression during semantic repetition priming in schizophrenia. *Psychiatry Res* 2010;181:114-120
15. Pyka M, Beckmann CF, Schöning S, Hauke S, Heider D, Kugel H, et al. Impact of working memory load on FMRI resting state pattern in subsequent resting phases. *PLoS One* 2009;4:e7198
16. Nelson B, Fornito A, Harrison BJ, Yücel M, Sass LA, Yung AR, et al. A disturbed sense of self in the psychosis prodrome: linking phenomenology and neurobiology. *Neurosci Biobehav Rev* 2009;33:807-817
17. Qiu MG, Ye Z, Li QY, Liu GJ, Xie B, Wang J. Changes of brain structure and function in ADHD children. *Brain Topogr* 2011;24:243-252
18. Broyd SJ, Demanuele C, Debener S, Helps SK, James CJ, Sonuga-Barke EJ. Default-mode brain dysfunction in mental disorders: a systematic review. *Neurosci Biobehav Rev* 2009;33:279-296
19. Assaf M, Jagannathan K, Calhoun VD, Miller L, Stevens MC, Sahl R, et al. Abnormal functional connectivity of default mode sub-networks in autism spectrum disorder patients. *Neuroimage* 2010;53:247-256
20. Barry RJ, Clarke AR, Hajos M, McCarthy R, Selikowitz M, Dupuy FE. Resting-state EEG gamma activity in children with attention-deficit/hyperactivity disorder. *Clin Neurophysiol* 2010;121:1871-1877
21. Cao X, Cao Q, Long X, Sun L, Sui M, Zhu C, et al. Abnormal resting-state functional connectivity patterns of the putamen in medication-naïve children with attention deficit hyperactivity disorder. *Brain Res* 2009;1303:195-206

22. Fair DA, Posner J, Nagel BJ, Bathula D, Dias TG, Mills KL, et al. Atypical default network connectivity in youth with attention-deficit/hyperactivity disorder. *Biol Psychiatry* 2010;68:1084-1091
23. Helps SK, Broyd SJ, James CJ, Karl A, Chen W, Sonuga-Barke EJ. Altered spontaneous low frequency brain activity in attention deficit/hyperactivity disorder. *Brain Res* 2010;1322:134-143
24. de Haan W, Pijnenburg YA, Strijers RL, van der Made Y, van der Flier WM, Scheltens P, et al. Functional neural network analysis in frontotemporal dementia and Alzheimer's disease using EEG and graph theory. *BMC Neurosci* 2009;10:101
25. Qi Z, Wu X, Wang Z, Zhang N, Dong H, Yao L, et al. Impairment and compensation coexist in amnestic MCI default mode network. *Neuroimage* 2010;50:48-55
26. Sorg C, Riedl V, Mühlau M, Calhoun VD, Eichele T, Läer L, et al. Selective changes of resting-state networks in individuals at risk for Alzheimer's disease. *Proc Natl Acad Sci U S A* 2007;104:18760-18765
27. Sambataro F, Blasi G, Fazio L, Caforio G, Taurisano P, Romano R, et al. Treatment with olanzapine is associated with modulation of the default mode network in patients with Schizophrenia. *Neuropsychopharmacology* 2010;35:904-912
28. Barry RJ, Clarke AR, Hajos M, McCarthy R, Selikowitz M, Bruggemann JM. Acute atomoxetine effects on the EEG of children with attention-deficit/hyperactivity disorder. *Neuropharmacology* 2009;57:702-707
29. Liddle EB, Hollis C, Batty MJ, Groom MJ, Totman JJ, Liotti M, et al. Task-related default mode network modulation and inhibitory control in ADHD: effects of motivation and methylphenidate. *J Child Psychol Psychiatry* 2011;52:761-771
30. Meindl T, Teipel S, Elmouden R, Mueller S, Koch W, Dietrich O, et al. Test-retest reproducibility of the default-mode network in healthy individuals. *Hum Brain Mapp* 2010;31:237-246
31. Zuo XN, Kelly C, Adelstein JS, Klein DF, Castellanos FX, Milham MP. Reliable intrinsic connectivity networks: test-retest evaluation using ICA and dual regression approach. *Neuroimage* 2010;49:2163-2177
32. Damaraju E, Phillips JR, Lowe JR, Ohls R, Calhoun VD, Caprihan A. Resting-state functional connectivity differences in premature children. *Front Syst Neurosci* 2010;4. pii: 23
33. Castellanos FX, Margulies DS, Kelly C, Uddin LQ, Ghaffari M, Kirsch A, et al. Cingulate-precuneus interactions: a new locus of dysfunction in adult attention-deficit/hyperactivity disorder. *Biol Psychiatry* 2008;63:332-337
34. Smyser CD, Inder TE, Shimony JS, Hill JE, Degnan AJ, Snyder AZ, et al. Longitudinal analysis of neural network development in preterm infants. *Cereb Cortex* 2010;20:2852-2862
35. Smith SM, Miller KL, Salimi-Khorshidi G, Webster M, Beckmann CF, Nichols TE, et al. Network modelling methods for FMRI. *Neuroimage* 2011;54:875-891
36. Beckmann CF, DeLuca M, Devlin JT, Smith SM. Investigations into resting-state connectivity using independent component analysis. *Philos Trans R Soc Lond B Biol Sci* 2005;360:1001-1013
37. Beckmann CF, Smith SM. Probabilistic independent component analysis for functional magnetic resonance imaging. *IEEE Trans Med Imaging* 2004;23:137-152
38. Filippini N, MacIntosh BJ, Hough MG, Goodwin GM, Frisoni GB, Smith SM, et al. Distinct patterns of brain activity in young carriers of the APOE-epsilon4 allele. *Proc Natl Acad Sci U S A* 2009;106:7209-7214
39. Uddin LQ, Kelly AM, Biswal BB, Xavier Castellanos F, Milham MP. Functional connectivity of default mode network components: correlation, anticorrelation, and causality. *Hum Brain Mapp* 2009;30:625-637
40. Damoiseaux JS, Rombouts SA, Barkhof F, Scheltens P, Stam CJ, Smith SM, et al. Consistent resting-state networks across healthy subjects. *Proc Natl Acad Sci U S A* 2006;103:13848-13853
41. Boly M, Phillips C, Tshibanda L, Vanhaudenhuyse A, Schabus M, Dang-Vu TT, et al. Intrinsic brain activity in altered states of consciousness: how conscious is the default mode of brain function? *Ann N Y Acad Sci* 2008;1129:119-129
42. Deuker L, Bullmore ET, Smith M, Christensen S, Nathan PJ, Rockstroh B, et al. Reproducibility of graph metrics of human brain functional networks. *Neuroimage* 2009;47:1460-1468
43. Chang C, Glover GH. Time-frequency dynamics of resting-state brain connectivity measured with fMRI. *Neuroimage* 2010;50:81-98
44. Born RT, Bradley DC. Structure and function of visual area MT. *Annu Rev Neurosci* 2005;28:157-189
45. Wolbers T, Zahorik P, Giudice NA. Decoding the direction of auditory motion in blind humans. *Neuroimage* 2011;56:681-687
46. Kiviniemi V, Starck T, Remes J, Long X, Nikkinen J, Haapea M, et al. Functional segmentation of the brain cortex using high model order group PICA. *Hum Brain Mapp* 2009;30:3865-3886